

# Phase separation in the Hubbard model

A. Macridin<sup>1</sup>, M. Jarrell<sup>1</sup>, Th. Maier<sup>2</sup>

<sup>1</sup>University of Cincinnati, Cincinnati, Ohio, 45221, USA

<sup>2</sup>Oak Ridge National Laboratory, Oak Ridge, Tennessee, 37831, USA

(Dated: July 1, 2020)

Phase separation in the Hubbard model is investigated with the dynamical cluster approximation. We find that it is present in the paramagnetic solution for values of filling smaller than one and at finite temperature when a positive next-nearest neighbor hopping is considered. The phase separated region is characterized by a mixture of a strongly correlated metallic and Mott insulating phases. Our results indicate that phase separation is driven by the formation of doped regions with strong antiferromagnetic correlations and low kinetic energy.

*Introduction* There is strong experimental evidence that high  $T_c$  materials are susceptible to charge inhomogeneities, such as stripes<sup>1</sup> or checkerboard modulation<sup>2</sup>. This discovery has spurred great theoretical interest in phase separation (PS) in models related to the cuprates, such as the Hubbard model which is believed to capture the low-energy physics of cuprate superconductors. It was argued by different authors that the charge instability displayed as PS in such simple models without long-range Coulomb interaction evolves into incommensurate charge ordering when the long-range repulsion is considered<sup>3</sup>. In this paper we present results on PS in the Hubbard model. We find that the paramagnetic asymmetric Hubbard model near half filling phase separates into undoped Mott liquid and doped Mott gas phases. The resulting Mott liquid-Mott gas phase diagram bears a strong resemblance to that of a classical liquid gas mixture.

Phase separation in the Hubbard and in the closely related t-J model has been intensively investigated. There is a general consensus that a t-J model with a large  $J/t$  separates into two phases, an undoped antiferromagnet (AF) and a hole rich region. However the results for realistic  $J/t < 1$  are controversial. Emery *et al.*<sup>4</sup>, Hellberg *et al.*<sup>5</sup> and Gimm *et al.*<sup>6</sup> report PS for all values of  $J/t$ . Others authors such as Putikka *et al.*<sup>7</sup> and Shih *et al.*<sup>8</sup> find no PS for small  $J/t$ . In the Hubbard model with only nearest-neighbor hopping, exact diagonalization<sup>9</sup> and Monte Carlo<sup>10</sup> calculations show no evidence of PS. These numerical results are consistent with the analytical results of G. Su's<sup>11</sup>, who show that there is no phase separation in the particle-hole symmetric Hubbard model. However, a large- $N$  investigation of this model in the infinite  $U$  limit shows PS when the next-nearest neighbor hopping  $t'$  is considered<sup>12</sup>. Phase separation in the Hubbard model at small doping was also found in a dynamical mean field calculation in the antiferromagnetic phase<sup>13</sup> and with variational cluster perturbation theory<sup>14</sup> in the antiferromagnetic and superconducting phases.

Phase separation is believed to be closely related with the antiferromagnetic order; a homogeneous doped system is unstable preferring to separate into an undoped antiferromagnetic region which lowers the exchange energy (maximizes the number of antiferromagnetic bonds)

and a rich doped phase with low kinetic energy. The driving force for PS in a t-J model when  $J/t$  is large will therefore be the desire to form undoped antiferromagnetic regions<sup>4</sup>. However in the Hubbard model we did not find PS for the values of parameters which are optimal for antiferromagnetic order in the undoped region. For instance, with DCA the maximum Néel temperature in the undoped system is obtained for  $U \approx 3/4W$ ,  $W = 8t$  being the electronic bandwidth, and for  $t' = 0$ . The later conditions can be understood by noticing that a finite  $t'$  introduces an antiferromagnetic exchange between the same sublattice sites, thus frustrating the antiferromagnetism. Nevertheless we find PS only for a  $U \geq W$  and a finite next-nearest-neighbor hopping  $t' \neq 0$ . Moreover, we find PS in the paramagnetic solution which shows that short range antiferromagnetic correlations are sufficient for the PS to take place. Presumably the PS is driven by the formation of weakly doped regions with strong antiferromagnetic correlations and low kinetic energy. The main culprit for the low value of the kinetic energy is the parameter  $t'$  with the right sign.

*Formalism* We use the Dynamical Cluster Approximation (DCA)<sup>15,16</sup> to explore the possibility of PS in the 2D Hubbard model, with

$$H = H_{kin} + H_{pot} \quad (1)$$

where

$$H_{kin} = -t \sum_{\langle ij \rangle, \sigma} c_{i\sigma}^\dagger c_{j\sigma} - t' \sum_{\langle\langle il \rangle\rangle, \sigma} c_{i\sigma}^\dagger c_{l\sigma} \quad (2)$$

$$H_{pot} = U \sum_i n_{i\uparrow} n_{i\downarrow}. \quad (3)$$

Here  $c_{i\sigma}^{(\dagger)}$  (creates) destroys an electron with spin  $\sigma$  on site  $i$  and  $n_{i\sigma}$  is the corresponding number operator.  $U$  is the on-site Coulomb repulsion. We consider hopping  $t$  between nearest-neighbors  $\langle ij \rangle$  and hopping  $t'$  between next-nearest-neighbors  $\langle\langle il \rangle\rangle$ . We show results for  $t = 1$ ,  $t' = 0.3$  and  $U = 8$ , which are realistic values for cuprates<sup>17,18,19</sup>. We find PS for values of the filling smaller than one, which for positive  $t'$  corresponds to the electron doped cuprates.

The DCA is an extension of the Dynamical Mean Field Theory (DMFT)<sup>20</sup>. The DMFT maps the lattice problem to an impurity embedded self-consistently in a host

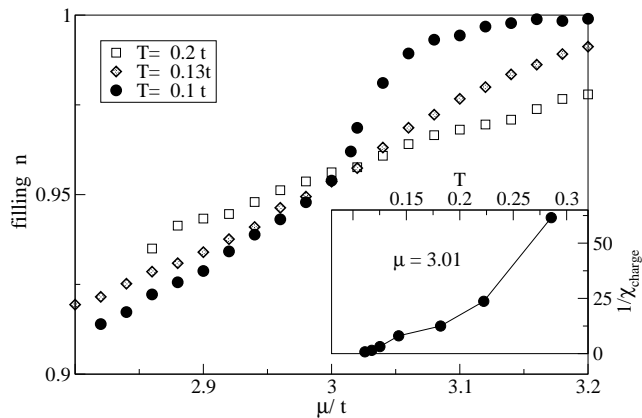


FIG. 1:  $N_c = 8$  results. Filling  $n$  versus chemical potential when  $T > T_c \approx 0.1 t$ . Inset: Inverse of the charge susceptibility  $\chi_{charge}$  versus temperature for fixed chemical potential  $\mu = \mu_c$ .

and therefore neglects spatial correlations. In the DCA we assume that correlations are short-ranged and map the original lattice model onto a periodic cluster of size  $N_c = L_c \times L_c$  embedded in a self-consistent host. Thus, correlations up to a range  $\xi \lesssim L_c$  are treated accurately, while the physics on longer length-scales is described at the mean-field level. We solve the cluster problem using quantum Monte Carlo (QMC)<sup>21</sup>. The cluster self-energy is used to calculate the properties of the host, and this procedure is repeated until a self-consistent convergent solution is reached.

Unlike most of the other numerical calculations on PS, which study systems with a fixed number of particles, our calculations are done in the grand canonical ensemble and in the thermodynamic limit. Therefore, unlike in finite cluster calculations, we do not encounter any particular difficulty associated with the small doping regime. Phase separation is explored by calculating the filling dependence on the chemical potential and the charge susceptibility (or compressibility),  $\chi_{charge} = \frac{dn}{d\mu}$ .

**Results** First we consider the case of an eight site ( $N_c = 8$ ) cluster. The filling as a function of the chemical potential is plotted in Fig. 1 for different temperatures<sup>30</sup>. Note that that at small doping with lowering temperature the charge susceptibility is increasing and diverging at a critical point ( $\delta_c, \mu_c, T_c$ ). The divergence of the charge susceptibility is illustrated in the inset. It is a clear indication that the filling is unstable and the system is subject to phase separation into regions with different hole density. The critical point is characterized by the temperature  $T_c \approx 0.10 t$  and the doping  $\delta_c \approx 4.5\%$ .

For temperatures smaller than  $T_c$  and for values of the chemical potential close to  $\mu_c$  the DCA calculation provides two distinct solutions for the same value of  $\mu$ . As mentioned before, the DCA equations are solved self-consistently starting with an initial guess for the self-energy, usually zero or that from a larger temperature or a perturbation theory result. In most of the situations

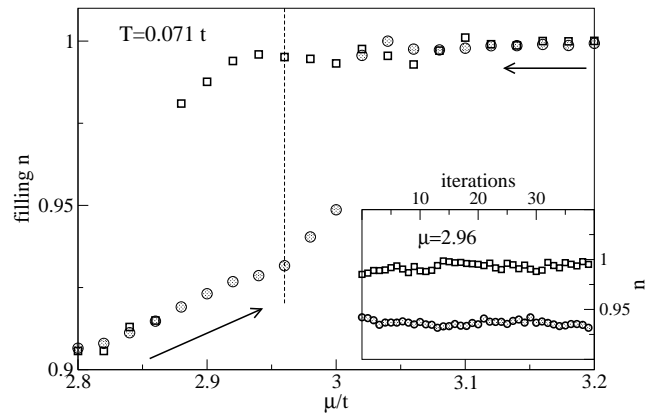


FIG. 2:  $N_c = 8$  results. Filling  $n$  versus chemical potential below  $T_c$ , at  $T = 0.071 t$ . Two solutions describing a hysteresis are found, one incompressible with  $n \approx 1$  (squares) and a doped one (circles). Inset: stability of the two solutions versus DCA iterations when  $\mu = 2.96t$  (middle of the hysteresis, corresponding to the dotted line in the main figure).

an unique solution is obtained independent of the starting guess. This is the case at doping values far from  $\delta_c$  such as 0% (undoped) or 10% doping. However, close to  $\mu_c$  we find that the final solution is dependent on the starting point. If one uses as the initial input the self-energy corresponding to the undoped solution ( $n = 1$ ), then  $n$  versus  $\mu$  will look as the upper curve (squares) in Fig. 2. On the other hand if the starting self-energy is the one corresponding to the large doped solution ( $n < 1$ ),  $n$  versus  $\mu$  will be described by the lower curve (circles) in Fig. 2. In both cases, the fully converged self energy of the previous point is used to initialize the calculation. Thus, below  $T_c$  the filling as a function of the chemical potential displays a hysteresis.

Simple thermodynamic ideas may be used to interpret these results. A hysteresis implies the existence of a metastable state and it is observed in many systems which suffer a first order transition, a common example being magnetization versus the applied magnetic field ( $M(H)$ ) in magnetic materials. However in the real systems, after a sufficient time, the fluctuations always drive the system to the stable solution (the equilibrium solution) and the hysteresis becomes a discontinuity characteristic to first order transitions. In our case, due to the mean-field coupling of the cluster to the effective medium, the hysteresis is stable. This is shown in the inset of Fig. 2 where a large number of iterations in the self-consistent process is considered.

By analogy with the liquid-gas system discussed below, we label the two states found for  $T < T_c$  as Mott liquid (ML) and Mott gas (MG). The Mott liquid is incompressible and insulating. Both the compressibility and doping of the ML are small and decrease with decreasing temperature. Its density of states at the Fermi surface develops a gap with lowering temperature characteristic of an insulator, as seen in Fig. 3-a. The MG is compress-

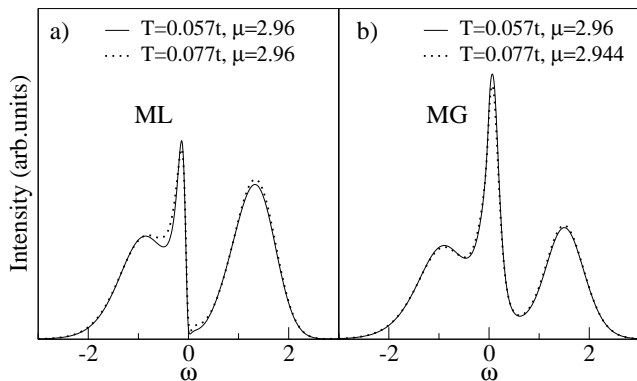


FIG. 3: a) DOS for ML solution at  $T = 0.077t$  (dotted line) and  $T = 0.057t$  (full line). b) DOS for MG solution at  $T = 0.077t$  (dotted line) and  $T = 0.057t$  (full line).

ible and metallic. The DOS is peaked at the chemical potential and increases with lowering temperature, see Fig. 3-b). Consistent with the narrow peak width, the MG is a strongly correlated state with a small value of the double occupancy ( $\langle n_{i\uparrow}n_{i\downarrow} \rangle/n \approx 0.04$  at  $T = 0.077t$ ) and strong AF correlations.

The stable solution below  $T_c$ , ML or MG, is the one with lower free energy,  $F = E - \mu N - TS$ . Unfortunately, due to the mean-field character of the DCA, the self-consistent solution is not necessarily the equilibrium state, and the QMC method does not allow the calculation of the entropy. Therefore the determination of the critical  $\mu$  where the jump in  $N(\mu)$  should take place is difficult to identify. However, the calculation of the energy provides valuable information about the transition mechanism. The energy plotted versus  $\mu$  displays a cusp at  $\mu_c$  when  $T = T_c$  (not shown). Below  $T_c$ , the energy is hysteretic. As can be seen in Fig. 4-a at fixed  $\mu$  the energy of the gas phase is much smaller, due to the large gain in kinetic energy (see Fig. 4-b) produced by the next-nearest-neighbor hopping  $t'$  as we will discuss. On the other hand, the term  $-\mu N$  will favor the ML state since it has a larger filling. In fact we find that the difference between  $E - \mu N$  for the two solutions is small, with the ML state being favored for larger values of  $\mu$ . When the chemical potential is decreased the system will be driven to the MG state by both the lower kinetic energy and the larger, presumably, entropy characteristic to MG state. Therefore, for  $T < T_c$ , we expect the jump in  $n$  will move to lower values of  $\mu$  as the temperature is lowered.

One can notice that a phase diagram with these characteristics bears a striking similarity to the phase diagram of a classical liquid gas mixture<sup>28</sup>, where  $\mu$  plays the role of pressure. A cartoon which summarizes our results and illustrates this similarity is shown in Fig 5. At high  $T$ ,  $n$  versus  $\mu$  is linear, since correlations are irrelevant. As the temperature is lowered,  $n(\mu)$  becomes nonlinear due to correlation effects. At  $T_c$ ,  $dn/d\mu$  diverges. Below  $T_c$  the hysteresis appears. Upon lowering the temperature the hysteresis broadens and the MG (ML) solution shifts

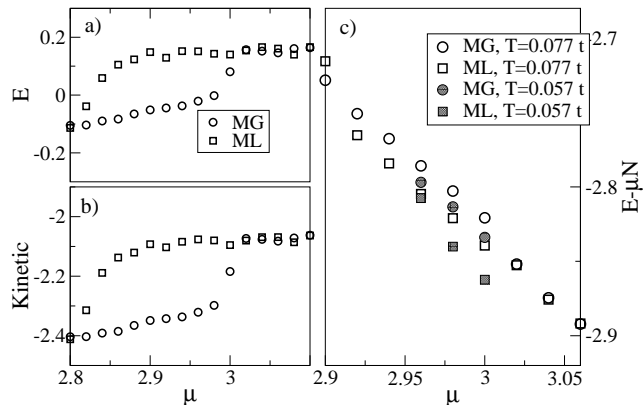


FIG. 4: Energy per site versus  $\mu$  for the two solutions: a) total energy  $E = \langle H \rangle$ , (see Eq. 1) at  $T = 0.077t$ , b) Kinetic energy  $= \langle H_{kin} \rangle$  (see Eq. 2) at  $T = 0.077t$ , c)  $E - \mu N$  at  $T = 0.077t$  and  $T = 0.057t$ .

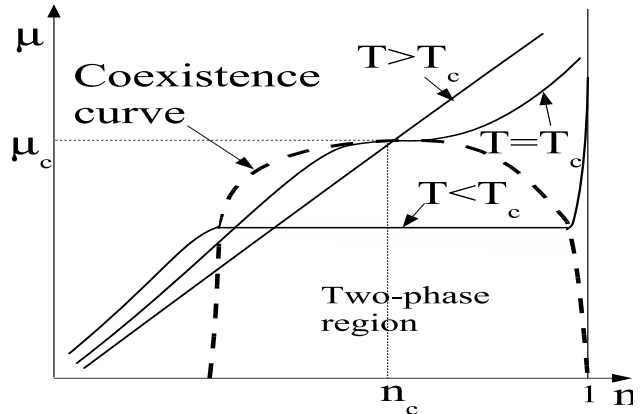


FIG. 5: Schematic representation of the phase diagram.

to slightly larger (smaller) dopings. As  $T \rightarrow 0$ , the entropy term becomes smaller and the chemical potential  $\mu_c$  where the jump takes place in the real solution should move to smaller values. If a fixed  $N$  is imposed when  $T < T_c$  in the two-phase parameter regime, the system will separate into distinct ML and MG regions.

Our calculations assume a paramagnetic host which implies that the range of possible AF order is restricted to the cluster size. For the  $N_c = 8$  cluster we find PS below the AF critical temperature  $T_N$ , the temperature where the AF spin susceptibility is diverging and the AF correlations range reaches the cluster size. Therefore it is important to address the role of AF correlations on phase separation. For this we investigate the behavior of the critical temperatures  $T_c$  and  $T_N$  when the cluster size increases. In the inset of Fig. 6 one can see that at 5% doping  $T_N$  decreases rapidly with increasing cluster size. On the other hand, the  $N_c = 12$  and  $N_c = 16$  site clusters display a divergent charge susceptibility roughly at the same  $T_c$  as the  $N_c = 8$  cluster,  $T_c \approx 0.1t$ , as shown in Fig. 6. The rapid decrease of  $T_N$  with  $N_c$  and the fact that  $T_c$  is nearly independent on  $N_c$  indicates that

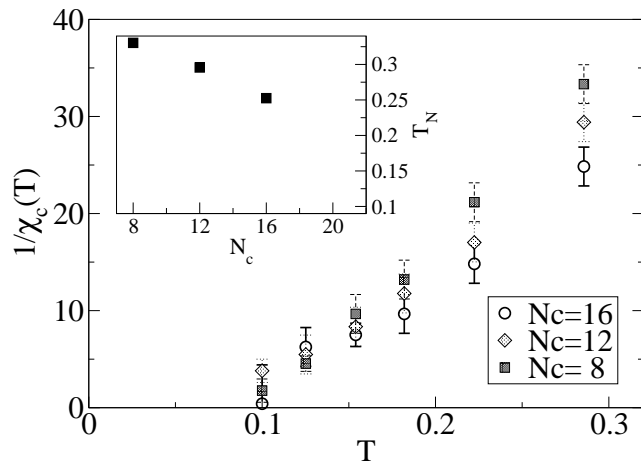


FIG. 6: Inverse charge susceptibility  $1/\chi_{charge}$  versus temperature for  $N_c = 8$  (squares),  $N_c = 12$  (diamonds) and  $N_c = 16$  (circles) site clusters at 5% doping. Inset: The AF temperature  $T_N$  versus cluster size  $N_c$ .

PS may persist in larger clusters at a temperature higher than  $T_N$  where the range of AF correlations is smaller than the cluster size. However, we must mention that the calculations on  $N_c = 12$  and  $N_c = 16$  clusters, close to the PS temperature, are extremely difficult. This region of parameter space is characterized by very strong critical behavior (presumably because a larger cluster implies a weaker hybridization with the effective medium, i.e. the results are less “mean-field”), a severe minus sign problem, and extremely large auto correlation times between measurements. Consequently, the error bar in the filling and the charge susceptibility is increasingly large for the low temperature points in Fig. 6 and it is difficult to obtain converged solutions. Therefore, besides a rough estimation of  $T_c \approx 0.1t$  it is difficult to make other quantitative estimates for the critical parameters. Low temperature calculations on larger clusters inside the critical region where a hysteresis is expected are not possible due to the severe sign problem which appears in the QMC calculation.

We find PS only when the next-nearest-neighbor hopping  $t' > 0$  and the filling  $n < 1$ . A finite  $t'$  in Hubbard and t-J models is known to give rise to a strong asymmetry between electron-doped ( $t' > 0$ ) and hole-doped ( $t' < 0$ ) systems<sup>18,22,23,24</sup>. In exact diagonalization studies on small clusters<sup>18,22,25,26,27</sup> it was shown that, due to the kinetic energy gain, the motion of holes caused by a positive  $t'$  stabilizes antiferromagnetic configurations<sup>18,22</sup>. Even though exact diagonalization on systems with four holes suggests that  $t'$  is not favorable to hole clustering<sup>22,26</sup> the tendency to PS was noted in Ref.<sup>22</sup>.

Our calculations also do not indicate hole clustering but rather formation of a 8% – 10% doped state with strong AF correlations and low-kinetic energy. Presumably for this value of the doping the effect of  $t'$  on the kinetic energy is the most significant.

For smaller values of  $t'$ , PS takes place at lower temperatures. For instance when  $t' = 0.1t$ , the system shows PS at  $T_c = 0.055t$  for the  $N_c = 8$  cluster. For  $U < W$  we found no sign of PS for temperatures above  $0.04t$ . The charge susceptibility behavior suggests that PS is not favored when  $t' < 0$  and  $n < 1$ , in agreement with exact diagonalization results<sup>22,29</sup> which show that in this case the effect of  $t'$  is to push the holes apart from each other.

Our results imply phase separation into two regions with different electronic density. However, even without considering long range order, we cannot exclude the possibility that PS competes with the formation of different charge patterns such as stripes or checkerboard. The investigation of these instabilities would require calculations on much larger clusters, able to commensurate these patterns, which are unfeasible at the moment.

It would be interesting to investigate the competition between PS and d-wave superconductivity in the Hubbard model. However this implies a region of the parameter space not accessible to our method. Calculations on clusters larger than  $N_c = 8$  show PS but the sign problem precludes access to temperatures where the superconductivity is expected. On the other hand, calculations on the small  $2 \times 2$  cluster, where the sign problem is mild, show d-wave superconductivity for finite  $t'$  but no definite evidence for PS, even though the charge susceptibility is strongly increased when a positive  $t'$  is considered<sup>24</sup>.

*Conclusions* With the DCA we show that the Hubbard model with a positive next-nearest-neighbor hopping displays PS for values of the filling slightly smaller than one. Our results suggest that the PS is driven by the desire to form slightly doped ( $\approx 8\% - 10\%$ ) regions with low-kinetic energy and strong antiferromagnetic correlations. The phase diagram is similar to that of the liquid-gas mixture, showing a second order critical point and a first order transition from a Mott gas to a Mott liquid state below  $T_c$ .

*Acknowledgment* We acknowledge useful discussions with S.R. White. This research was supported by NSF Grants DMR-0312680 and DMR-0113574, by CMSN grant DOE DE-FG02-04ER46129 and was supported in part by NSF cooperative agreement SCI-9619020 through resources provided by the San Diego Supercomputer Center. Part of the computation was also performed at the Center for Computational Sciences at the Oak Ridge National Laboratory.

<sup>1</sup> J. M. Tranquada, B. J. Sternlieb, J. D. Axe, Y. Nakamura, S. Uchida, Nature (London) **375**, 561 (1995); J.

M. Tranquada, J. D. Axe, N. Ichikawa, Y. Nakamura, S. Uchida and B. Nachumi, Phys. Rev. B **54**, 7489 (1996);

- J. M. Tranquada, J. D. Axe, N. Ichikawa, A. R. Moodenbaugh, Y. Nakamura, and S. Uchida, *Phys. Rev. Lett.* **78**, 338 (1997).
- <sup>2</sup> J. E. Hoffman, E. W. Hudson, K. M. Lang, V. Madhavan, H. Eisaki, S. Uchida, and J. C. Davis, *Science* **295**, 466 (2002); C. Howald, H. Eisaki, N. Kaneko, M. Greven, and A. Kapitulnik, *Phys. Rev. B* **67**, 014533 (2003); Michael Vershinin, Shashank Misra, S. Ono, Y. Abe, Yoichi Ando, and Ali Yazdani, *Science* **303**, 1995 (2004); T. Hanaguri, C. Lupien, Y. Kohsaka, D.-H. Lee, M. Azuma, M. Takano, H. Takagi, J. C. Davis, *Nature (London)* **430**, 1001 (2004); K. McElroy, D. H. Lee, J. E. Hoffman, K. M. Lang, J. Lee, E. W. Hudson, H. Eisaki, S. Uchida, and J. C. Davis, *Phys. Rev. Lett.* **94**, 197005 (2005).
- <sup>3</sup> S.A. Kivelson and V.J. Emery, in *Strongly Correlated Electronic Materials: The Los Alamos Symposium 1993*, edited by K. S. Bedell, Z. Wang, and D. E. Meltzer (Addison-Wesley, Redwood City, 1994); G. Seibold, C. Castellani, C. Di Castro, and M. Grilli, *Phys. Rev. B* **58**, 13506 (1998).
- <sup>4</sup> V. J. Emery, S. A. Kivelson and H. Q. Lin, *Phys. Rev. Lett.* **64**, 475, (1990).
- <sup>5</sup> C. S. Hellberg and E. Manousakis, *Phys. Rev. Lett.* **78**, 4609, (1997); Jung Hoon Han, Qiang-Hua Wang, and Dung-Hai Lee, *Int. J. Mod. Phys. B* **15**, 1117 (2001).
- <sup>6</sup> Tae-Hyoung Gimm and Sung-Ho SuckSalk, *Phys. Rev. B* **62**, 13930, (2000).
- <sup>7</sup> W. O. Putikka and M. U. Luchini, *Phys. Rev. B* **62**, 1684, (2000).
- <sup>8</sup> C. T. Shih, Y. C. Chen and T. K. Lee, *Phys. Rev. B* **57**, 627, (1998).
- <sup>9</sup> A. Moreo, D. Scalapino, and E. Dagotto, *Phys. Rev. B* **43**, 11442, (1991).
- <sup>10</sup> Federico Becca, Massimo Capone and Sandro Sorella, *Phys. Rev. B* **62**, 12700, (2000).
- <sup>11</sup> Gang Su, *Phys. Rev. B* **54**, R8281, (1996).
- <sup>12</sup> Lew Gehlhoff, *J. Phys: Condensed Matter* **8**, 2851 (1996).
- <sup>13</sup> R. Zitzler, Th. Pruschke, and R. Bulla, *Eur. Phys. J. B* **27**, 473, (2002).
- <sup>14</sup> M. Aichhorn and E. Arrigoni, *Europhys. Lett.* **71**, 117 (2005); M. Aichhorn, E. Arrigoni, M. Potthoff and W. Hanke, preprint, cond-mat/0511460 (2005).
- <sup>15</sup> M. H. Hettler, A. N. Tahvildar-Zadeh, M. Jarrell, T. Pruschke, and H. R. Krishnamurthy, *Phys. Rev. B* **58**, R7475 (1998); M. H. Hettler, M. Mukherjee, M. Jarrell, and H. R. Krishnamurthy, *Phys. Rev. B* **61**, 12739 (2000); T. Maier, M. Jarrell, T. Pruschke, and J. Keller, *Eur. Phys. J. B* **13**, 613 (2000).
- <sup>16</sup> T. Maier, M. Jarrell, T. Pruschke, and M. H. Hettler, *Rev. Mod. Phys.* **77**, 1027 (2005).
- <sup>17</sup> H. Eskes, G. A. Sawatzky, and L. Feiner, *Physica C*, **160**, 424 (1989).
- <sup>18</sup> T. Tohyama and S. Maekawa, *J. Phys. Soc. Japan*, **59**, 1760, (1990); T. Tohyama and S. Maekawa, *Phys. Rev. B* **49**, 3596 (1993).
- <sup>19</sup> Mark S. Hybertsen, E. B. Stechel, M. Schluter, and D. R. Jennison, *Phys. Rev. B* **41**, 11068, (1990).
- <sup>20</sup> Th. Pruschke, M. Jarrell, and J.K. Freericks, *Advances in Physics* **44**, 187 (1995); A. Georges G.Kotliar, W.Krauth and M.Rozenberg, *Rev.Mod.Phys.* **68**, 13 (1996).
- <sup>21</sup> M. Jarrell, Th. Maier, C. Huscroft, and S. Moukouri, *Phys.Rev. B* **64**, 195130 (2001).
- <sup>22</sup> R. J. Gooding, K. J. E. Vos and P. W. Leung, *Phys. Rev. B* **50**, 12866, (1994).
- <sup>23</sup> T. Tohyama and S. Maekawa, *Supercond. Sci. Technol.* **13**, R17, (2000)
- <sup>24</sup> A. Macridin, M. Jarrell, Th. Maier, and G. A. Sawatzky, *Phys. Rev. B* **71**, 134527, (2005).
- <sup>25</sup> J. A. Riera, *Phys. Rev. B* **40**, R833, (1989)
- <sup>26</sup> Toshihiro Itoh, Masao Arai, and Takeo Fujiwara, *Phys. Rev. B* **42**, R4834 (1990).
- <sup>27</sup> Eduardo Gagliano, Silvia Bacci, and Elbio Dagotto, *Phys. Rev. B* **42**, 6222, (1990).
- <sup>28</sup> H.E. Stanley, *Introduction to Phase Transitions and Critical Phenomena*, (Oxford Univ. Press, New York, 1971).
- <sup>29</sup> T. Tohyama and S. Maekawa, *Phys. Rev. B* **67**, 092509 (2003).
- <sup>30</sup> The statistical error bars on the densities are of the order of the symbol size or smaller. In the DCA, the error bars for the lattice susceptibilities can only be obtained by repeated runs. Due to the computational expense of this procedure, it was generally not done, except where specified.